Changes in trait covariance along an orographic moisture gradient reveal the relative importance of light- and moisture-driven trade-offs in subtropical rainforest communities

Alison Brown[1], **Donald W. Butler**[2] (iD), **Julian Radford-Smith**[1] (iD) **and John M. Dwyer**[1] (iD)

[1]School of Biological Sciences, The University of Queensland, St Lucia, Qld 4072, Australia; [2]College of Law, Australian National University, Canberra, ACT 2600, Australia

Author for correspondence:
John M. Dwyer
Email: j.dwyer2@uq.edu.au

Summary

- A range of functional trait-based approaches have been developed to investigate community assembly processes, but most ignore how traits covary within communities.
- We combined existing approaches – community-weighted means (CWMs) and functional dispersion (FDis) – with a metric of trait covariance to examine assembly processes in five angiosperm assemblages along a moisture gradient in Australia's subtropics. In addition to testing hypotheses about habitat filtering along the gradient, we hypothesized that trait covariance would be strongest at both ends of the moisture gradient and weakest in the middle, reflecting trade-offs associated with light capture in productive sites and moisture stress in dry sites.
- CWMs revealed evidence of climatic filtering, but FDis patterns were less clear. As hypothesized, trait covariance was weakest in the middle of the gradient but unexpectedly peaked at the second driest site due to the emergence of a clear drought tolerance–drought avoidance spectrum. At the driest site, the same spectrum was truncated at the 'avoider' end, revealing important information about habitat filtering in this system.
- Our focus on trait covariance revealed the nature and strength of trade-offs imposed by light and moisture availability, complementing insights gained about community assembly from existing trait-based approaches.

Introduction

An important aim of plant ecology is to understand how biotic and abiotic conditions structure the composition of plant communities (Weiher & Keddy, 1995; McGill *et al.*, 2006). Whereas processes such as dispersal limitation influence local community composition (Kraft *et al.*, 2015), habitat filtering is a major driver of compositional turnover along steep environmental gradients that span relatively short geographic distances. The importance of habitat filtering is strongly supported by trait-based studies showing how the ecological and physiological strategies of successful species change systematically along gradients of moisture availability (e.g. Cornwell & Ackerly, 2009) and temperature (e.g. Laughlin *et al.*, 2011).

Trait-based studies typically view communities as distributions of trait values and then assess how moments of these distributions change along gradients. Univariate trait analyses examine the abundance-weighted (or 'community-weighted') distributions of one trait at a time, typically focusing on means and variances of these distributions. For example, declines in the community-weighted mean (CWM) of leaf area along an aridity gradient may be interpreted as abiotic filtering (Cornwell & Ackerly, 2009) where having larger leaves is assumed to be a less viable

strategy in drier environments, on average. Whereas CWMs have revealed important insights about habitat filtering across a range of systems globally, the approach implicitly assumes an optimum trait value in each location (Shipley *et al.*, 2006; Laughlin *et al.*, 2012), even though trait variation within communities is often larger than between communities (Westoby *et al.*, 2002; Bruelheide *et al.*, 2018).

Multivariate trait-based approaches (Villéger *et al.*, 2008; Laliberté & Legendre, 2010; Blonder *et al.*, 2014) focus on how the volume, spacing, or dispersion of multidimensional trait distributions change along environmental gradients, with the common expectation that multi-trait functional diversity is high under favourable climatic conditions and declines as conditions become drier or colder (Spasojevic *et al.*, 2014). Though many of these multivariate approaches focus directly on trait variation within communities, they can be difficult to interpret without also examining the dispersion patterns of individual traits, and they may even obscure assembly processes if individual traits have opposing dispersion patterns along environmental gradients (Spasojevic & Suding, 2012). Both univariate and multivariate approaches also reveal little information about trade-offs operating *within* communities.

Trait variation emerges within communities because trait-based trade-offs permit multiple viable strategies to coexist in any

given environment (Marks & Lechowicz, 2006; Falster *et al.*, 2017; Messier *et al.*, 2017). When species are viewed as coordinated ensembles of trait values, trade-offs are evident as differential coordination of multiple traits, and at the community scale this can generate informative trait covariance among species (Dwyer & Laughlin, 2017). Strong trait covariance is expected to emerge in productive systems where light-driven trade-offs are strong (Falster *et al.*, 2017) and in systems limited by other resources, such as water (Dwyer & Laughlin, 2017; Sanaphre-Villanueva *et al.*, 2022). For example, in mesic rainforests, trade-offs associated with fast growth in high light vs survival in low light allow many tree species to coexist (Sterck *et al.*, 2006, 2011). Furthermore, tall individuals that reach the canopy attain access to plentiful light but must overcome the challenges of structural support (Niklas, 1992) and increasing hydraulic resistance associated with long xylem path lengths (Ryan & Yoder, 1997; Koch *et al.*, 2004), resulting in additional trade-offs related to species' potential heights in these productive mesic environments (Hietz *et al.*, 2017).

In drier forests, a spectrum of drought-resistance strategies emerges from trade-offs between hydraulic efficiency and hydraulic safety (Sterck *et al.*, 2011), though not all species conform strongly to this trade-off globally (Gleason *et al.*, 2016; Liu *et al.*, 2021). Hydraulic efficiency permits faster water transport during favourable periods but increases the risk of embolism during extended dry periods, whereas hydraulic safety sacrifices water transport efficiency to reduce embolism risk (Baas *et al.*, 2004). At the extremes of this trade-off spectrum are species that tolerate drought with safe strategies (e.g. low maximum heights, small vessel lumens, high wood density, and small, toughened leaves) and those with efficient hydraulics that avoid embolism risk in droughts by shedding leaves and storing water (Eamus, 1999; Méndez-Alonzo *et al.*, 2013; Pineda-García *et al.*, 2013).

These light- and moisture-driven trade-offs are not mutually exclusive (Sterck *et al.*, 2006; Markesteijn *et al.*, 2011; Liu *et al.*, 2019), but trait-based evidence of their relative importance can likely be interpreted within the resource context of each community (Funk & Cornwell, 2013). To this end, this study focuses on five communities of rainforest angiosperms distributed along a steep orographic moisture gradient in Australia's subtropics. We combine detailed floristic surveys with seven functional traits that describe species' light-acquisition and hydraulic strategies. We start by using existing trait-based approaches to infer community assembly processes. We then examine what additional information can be obtained from a focus on within-community trait covariance, including a simple and unbiased metric of trait covariance borrowed from evolutionary biology. Specifically, we assess support for the following hypotheses:

(**1**) CWMs of certain traits vary systematically along the moisture gradient consistent with habitat filtering.

(**2**) Multivariate functional diversity (functional dispersion (FDis)) increases with mean annual precipitation consistent with habitat filtering. As a result, it is lower than expected under random assembly in the driest site and higher than expected at the wettest site.

(**3**) Trait covariance peaks at the dry and wet ends of the moisture gradient, reflecting strong trait-based trade-offs associated

with moisture stress in dry sites and light capture in productive sites. As a result, trait covariance is higher than expected under random assembly at either end of the gradient and lower than expected in the middle of the gradient.

Materials and Methods

Study site

The study was conducted in the Bunya Mountains National Park (Supporting Information Fig. S1), 160 km west northwest of Brisbane, the capital city of Queensland. The national park varies in elevation from 550 m to 1100 m above sea level. Orographic rainfall and fog result in a gradient of declining precipitation from highest elevation to lowest (Butler, 2004), with the steepest declines on the western side of the range. Rainfall is summer dominant, and the driest month is August (late winter) on average (BOM, 2021a).

Surveying communities

Five rainforest communities (Table 1) were surveyed, spanning a gradient of mean annual precipitation of 255 mm yr^{-1}. From wettest (965 mm yr^{-1}) to driest (710 mm yr^{-1}), the vegetation types can be classified as complex notophyll vine forest (CNVF) with *Araucaria* species, Araucarian notophyll vine forests, microphyll vine forests, semi-evergreen vine thicket (SEVT), and SEVT with *Brachychiton rupestris* (Queensland Herbarium, 2015). All communities were located on fertile loam soils derived from Cainozoic basalt (Main Range Volcanics; 28.1–15.97 million years ago; Raymond *et al.*, 2012). Though selective logging occurred on the mountain top and eastern slopes up until 60 yr ago, our plots comprised primary canopy species and there were no signs of selective logging.

Survey data consisted of three previously surveyed plots and two newly surveyed plots. The existing data included three 1 ha plots established by Butler (2004) at different elevations and aspects (high, mid east, and mid west). In Butler's (2004) survey, the location and size of all woody, self-supporting individuals > 2 m tall were recorded. All stems were mapped, identified to species level, and their girth measured at breast height (1.3 m above ground). We subsampled four 25 m × 25 m subplots from the corners of these existing plots to match the sampling design to our new plots. Only individuals ≥ 3 cm stem diameter were included to capture individuals that had transitioned past the sapling stage. This subsampling approach captured 87.5% of species recorded across all three 1 ha plots surveyed by Butler (2004) and returned very similar abundance rankings of species in each plot. Two additional communities were surveyed on the lower eastern and western slopes to extend the coverage of the orographic moisture gradient into the driest parts of the national park (low east and low west). In these two additional communities, four 25 m × 25 m subplots were sampled in the same arrangement as those subsampled from Butler's (2004) data. In each subplot, the stem diameter and identity of all self-supporting woody individuals ≥ 3 cm was recorded.

Table 1 Elevation, coordinates and climate variables for each of the five sites extracted from topographically adjusted climate layers (Harwood *et al.*, 2016) and ANUCLIMATE 2.0 (frost days; Hutchinson *et al.*, 2022).

Site	Elevation (m)	Latitude	Longitude	Mean T_{min} (°C)	Mean T_{max} (°C)	Mean annual frost days[a]	Mean annual precip. (mm)	Annual total water deficit (mm)[b]	Precip. seasonality (ratio)[c]
High	1050	−26.8702	151.584	10.109	21.336	58.5	965.45	−243.40	−0.063
Mid east	950	−26.8662	151.5926	10.340	21.976	49.3	912.21	−312.84	−0.031
Mid west	950	−26.8309	151.5405	10.629	22.301	43.0	829.62	−334.47	0.034
Low east	**625**	**−26.8582**	**151.6479**	**11.110**	**24.162**	**34.1**	**759.65**	**−539.90**	**0.043**
Low west	**595**	**−26.8358**	**151.4994**	**11.198**	**24.445**	**36**	**709.60**	**−606.36**	**0.137**

Newly surveyed sites are shown in bold.
[a]Mean number of days per year with minimum temperatures ≤ 2°C.
[b]Difference between mean annual precipitation and mean annual potential evaporation.
[c]Spring vs Autumn.

Climate data

The moisture gradient was quantified using topographically adjusted climate data (100 m grid cells) developed by Harwood *et al.* (2016). Values of mean annual precipitation (MAP) were extracted for each of the plot locations using the extract() function from the RASTER package (Hijmans, 2021). All climate variables were highly correlated, and we selected mean annual rainfall (millimetres) to represent the moisture gradient. We also extracted the mean annual number of frost days for each site from ANUCLIMATE 2.0 (Hutchinson *et al.*, 2022).

Trait sample collection and measurement

Traits were chosen to capture expected light- and moisture-driven trade-offs, while being feasible to measure on many species across multiple sites (Table 2). Leaf, branch, and wood samples were collected from the Bunya Mountains where possible. Additional branch samples were collected from the nearby Yarraman State Forest. Branch samples were taken from mature specimens located along sun-exposed forest edges (e.g. where roads had been cut through primary forest) using telescopic pole pruners.

Lamina area, specific leaf area, and leaf dry matter content Four sun-exposed branches per species were collected from different individuals and stored in wetted plastic garbage bags during transport. In the laboratory, branches were recut under deionized water and left overnight to rehydrate in the dark. Following rehydration, four leaves from each individual were selected to measure lamina area and fresh mass. In the case of compound leaves, measurements were taken on leaflets. Leaves (or leaflets) were scanned on a flatbed scanner (CanoScan LiDE 700F; Canon, Tokyo, Japan) and their area calculated using IMAGEJ (Schneider *et al.*, 2012). Fresh mass was recorded with an analytical balance (GR-200; A&D Co. Ltd, Tokyo, Japan). Leaves (or leaflets) were dried to constant mass at 70°C for 3 d, and their dry mass recorded. Specific leaf area (SLA; lamina area/dry mass) and leaf dry matter content (LDMC; dry mass/fresh mass) were then calculated for each individual leaf or leaflet.

Petiole vessel traits Petioles from three individuals of each species were collected in the field and stored in the fixative formaldehyde acetic acid. In the laboratory, the samples were rinsed twice with distilled water and once with phosphate buffered saline (PBS) before being stored in PBS. Samples were cryoprotected in 15% buffered sucrose, followed by 30% buffered sucrose, before being mounted in optimal cutting temperature compound and frozen on dry ice. Petiole samples were sectioned using a cryostat (CryoStar NX70; Thermo Fisher Scientific, Waltham, MA, USA) at 10 µm section thickness. Sectioned samples were stained with 0.1% toluidine blue in 1% sodium acetate buffer solution and mounted with coverslips using DePeX. Vessels were imaged with a light microscope at ×40 magnification. For each sample, three distinct bundles of xylem vessels were imaged. Xylem vessel wall thickness and lumen diameter were measured using IMAGEJ (Schneider *et al.*, 2012). Within each bundle, five adjacent vessels were measured to capture within-individual variation. For each vessel, the lumen breadth b was calculated as the average of the widest and narrowest lumen measurements, and vessel wall thickness t was calculated as the average of three measurements per vessel (Fig. S2). From these measurements we calculated species-level averages for lumen breadth (as an indicator of hydraulic efficiency) and wall thickness/lumen breadth t/b (as an indicator of vessel reinforcement; Blackman *et al.*, 2018).

Wood density Wood density was measured on branch samples (5–7 cm long, avoiding bifurcating tissue), from three individuals of each species. Bark was removed and the water displacement method was used to estimate fresh volume. Samples were dried for 3 d and weighed to determine dry mass. Owing to limitations of the drying oven at the time of measurement, these samples were dried at 80°C, which may not be hot enough to dry wood to constant mass (Williamson & Wiemann, 2010). We therefore redried 52 samples from a range of different plant families at 105°C in a different oven, recalculated wood density, and fitted a linear regression between the values obtained from 80°C (*x*) and 105°C (*y*) ($R^2 = 0.9992$; Fig. S3). We then used this regression to adjust all wood density values originally obtained using 80°C.

Table 2 The seven functional traits measured in this study and their relevance to light-driven and moisture-driven trade-offs in rainforests generally (including seasonally dry forests).

Functional trait	Relevance to light-driven trade-offs	Relevance to moisture-driven trade-offs
Specific leaf area (SLA; $mm^2 mg^{-1}$)	Positively related to growth rate under high light and negatively related to survival under low light (Sterck et al., 2006); negatively associated with closed-canopy situations in mesic forests (Poorter, 2009)	In dry forests, evergreen species tend to have long-lived, low-SLA leaves, and drought-deciduous species tend to have high-SLA leaves to facilitate rapid re-leafing and to recoup foregone growth opportunities (Markesteijn et al., 2011)
Leaf dry matter content (LDMC; $mg mg^{-1}$)	Positively associated with closed-canopy situations in mesic forests (Poorter, 2009) suggesting a role in shade tolerance	Negatively related to leaf turgor loss point (Bartlett et al., 2012), i.e. positively related to the maintenance of leaf turgor
Lamina area (mm^2)	Light interception in mesic forests (Wright et al., 2017)	Large leaves are difficult to cool under warm, dry conditions (Leigh et al., 2017; Wright et al., 2017); Small leaves have higher major vein densities and thus lower hydraulic vulnerability (Scoffoni et al., 2011) but see (Blackman et al., 2018)
Wood density ($g cm^3$)	High wood density is associated with high survival in low-light environments but slow growth in high-light environments (Wright et al., 2010)	Negatively related to sapwood water storage and capacitance (De Guzman et al., 2020) and positively related to hydraulic safety (Liang et al., 2021)
Maximum height (H_{max}; m)	Taller species intercept more light than co-occurring shorter species (King, 1990; Westoby et al., 2002)	Long path lengths increase hydraulic resistance due to gravity and friction (Ryan & Yoder, 1997)
Vessel lumen breadth (µm; measured in petioles)	Taller-growing species have larger vessels to overcome resistance from longer path lengths (Zach et al., 2010; Liu et al., 2019)	Positively related to hydraulic efficiency (Tyree & Zimmerman, 2002)
Vessel wall thickness/lumen breadth (t/b; measured in petioles)	High values may mitigate hydraulic vulnerabilities associated with long path lengths (Blackman et al., 2010, 2018)	Negatively related to leaf hydraulic vulnerability to drought (Blackman et al., 2010, 2018)

Maximum heights Maximum heights H_{max} for each species were obtained from Harden et al. (2006), the most authoritative reference for Australian subtropical rainforest species.

Calculating species means and gap filling from existing data sources Individual trait values were averaged by species, and the average was applied to each occurrence of each species (e.g. all occurrences of *Acalypha capillipes* were given a lamina area of 80.3 mm^2). We recognize that intraspecific trait variation likely contributes to trait dispersion and covariance, but it was not possible to collect sun-exposed branches from mature individuals of each species in each site. Using mean trait values for species was supported by exploratory variance components analyses indicating that > 70% of variation in each trait was among species (rather than within species), except for t/b in which 55% of variation was between species (Fig. S4). Lamina area, SLA, and t/b were log-transformed, and maximum height and lumen breadth were square-root-transformed to approximate normal distributions. Gymnosperms were excluded from analyses because they lack xylem vessel elements.

In total, we collected samples and measured all seven traits for 58 species across the five sites. Traits could not be safely collected from the giant stinging tree, *Dendrocnide excelsa*. For this species, SLA was obtained from McCarthy et al. (2019), lamina area from Lowman & Box (1983), and wood density from Ilic et al. (2000). For the remaining traits, values of its close relative, *Dendrocnide photinophylla* (which could be measured safely in this study), were used. For all traits, we achieved at least 93% coverage of individuals and at least 73% coverage of species in each site (Table S1).

Statistical analyses

All statistical analyses were conducted in R v.4.1.1 (R Development Core Team, 2021). Data from the four subplots in each community were pooled prior to statistical analyses. For all analyses, we weighted species by their pooled abundance in each site instead of weighting by basal area, which biases towards species that can attain larger sizes over smaller-statured strategies that are equally viable in a given environment. Furthermore, we log-transformed abundances to reduce the influence of hyperabundant species that were especially evident in drier communities (e.g. *Backhousia angustifolia* and *A. capillipes*).

To address the first hypothesis, we examined how mean trait values per site varied along the moisture gradient. Rather than precalculating CWMs for each trait, species' trait values in each site were treated as separate observations and were weighted by their relative log(abundance + 1) in each site. These weighted trait values were then modelled as a function of mean annual rainfall using linear mixed effects models (lmer() function from the LME4 package; Bates et al., 2015) with site included as a random effect to reflect the nesting of trait values within each site. This parameterization effectively modelled the abundance-weighted trait mean of each site, while accounting for trait variation within sites. We fitted separate lmer() models to calculate the average percentage of trait variance occurring within sites (compared with between sites). These variance components were necessarily calculated using unweighted trait values because weighting of observations scales the estimate of residual (within-site) variance during model fitting (Bates et al., 2015).

To address the second hypothesis, we calculated the multivariate FDis (Laliberté & Legendre, 2010) weighted by each species'

log(abundance + 1) in each site using the FDindexes() wrapper function from the FUNDIV package (Bartomeus, 2019). We chose FDis over other indices of functional diversity because it is a direct measure of multivariate trait variation, rather than a measure of trait spacing or trait space volume.

To address the third hypothesis, a measure of overall trait covariance was first calculated using eigenanalysis on each site's abundance-weighted trait correlation matrix. Specifically, the PCA() function from the FACTOMINER package (Lê *et al.*, 2008) was applied to standardized trait values (mean of 0, SD = 1), with the rows (species) weighted by their log(abundance + 1) in each site. From each principal component analysis (PCA) we extracted the seven eigenvalues and calculated an unbiased estimate of eigenvalue variance (Cheverud *et al.*, 1989), as follows:

$$\mathrm{Var}(\lambda) = \mathrm{Var}(\lambda_{\mathrm{raw}}) - \frac{M-1}{N}$$

where λ_{raw} are the eigenvalues, M is the number of traits, and N is the number of species included in each PCA. Subtraction of $(M-1)/N$ is required to remove sampling error because even random draws of species are expected to have nonzero trait correlation when comparing assemblages with differing numbers of species (Cheverud *et al.*, 1989). High $\mathrm{Var}(\lambda)$ indicates that the first eigenvalue is dominant (strong covariance among many traits) and low $\mathrm{Var}(\lambda)$ indicates the opposite (Boucher *et al.*, 2013). We also fitted an unweighted 'global' PCA to all species recorded across all five sites. PCA biplots were generated to visually compare vector loadings (and hence trade-offs) across sites (Lohbeck *et al.*, 2015), and between the global PCA and each site.

To compare the observed values of FDis and $\mathrm{Var}(\lambda)$ with those expected under random community assembly, we generated 'expected' FDis and $\mathrm{Var}(\lambda)$ distributions under two randomization procedures. The first simply shuffled all recorded individuals among sites. Specifically, we generated 999 randomizations using the permatfull() function from the VEGAN package (Oksanen *et al.*, 2021) by shuffling individuals (not individuals AND incidences) with fixed column sums (species total abundances). The second procedure was more constrained, and hence realistic. It maintained the observed number of individuals per species, observed site richness, and observed matrix fill (i.e. the observed number of zeros in the matrix). For this procedure we generated 999 randomizations using the permatswap() function from the VEGAN package (Oksanen *et al.*, 2021) with the 'swsh' algorithm and fixed column sums (species total abundances).

We plotted the observed values of FDis and $\mathrm{Var}(\lambda)$ over the distributions of the random expectations and calculated the percentiles where observed values sit on these distributions. Though we did not assume normal distributions and calculate *P*-values, percentiles < 0.025 and > 0.975 can be interpreted as significant ($\alpha = 0.05$).

Results

Consistent with the first hypothesis, the CWMs for five of the seven traits were significantly related to MAP. Leaf area, lumen breadth, and maximum height were positively related (Fig. 1a,d, g), whereas wood density and t/b were negatively related to MAP (Fig. 1e,f). Regardless of the strength of CWM ~ MAP relationships, at least 79% of trait variance remained unexplained within sites (Fig. 1).

Though FDis was lowest in the driest site, it did not increase consistently with MAP as hypothesized (Fig. 2a). Compared with unconstrained shuffling of individuals, all but the middle site had significantly lower FDis than expected. Compared with the more constrained randomization procedure, only FDis at driest site was significantly different (percentile = 0.02; Fig. 2a).

There was mixed support for the third hypothesis. As expected, $\mathrm{Var}(\lambda)$ was lowest in the middle of the gradient but did not peak at the driest and wettest ends of the gradient. Instead, $\mathrm{Var}(\lambda)$ peaked in the second driest site (Fig. 2b). Compared with unconstrained shuffling of individuals, only $\mathrm{Var}(\lambda)$ values for the middle three sites (low east, mid west, and mid east) differed significantly. Respectively, these were higher, lower, and lower than expected. Compared with the more constrained procedure, only $\mathrm{Var}(\lambda)$ for the middle site differed significantly (percentile = 0.02). $\mathrm{Var}(\lambda)$ for the second driest site was close to being significantly higher than expected under the constrained procedure (percentile = 0.91; Fig. 2b).

The PCA including all species (Fig. 3a) had a $\mathrm{Var}(\lambda)$ of 1.769, suggesting strong trait coordination across the species pool. On the first principal component (PC1; 55.9%), all traits except SLA had loadings > |0.35| with signs consistent with PC1 being a spectrum from safe hydraulic strategies (shorter growing, dense wood, small leaves, reinforced leaf vessels, and small lumen breadths) to taller-growing strategies with efficient hydraulics. PC2 (17%) was most strongly loaded by SLA (+) and LDMC (−), reflecting the leaf economics spectrum.

At the driest site (710 mm yr^{-1}), PC1 (51.5%) was strongly loaded by maximum height (+), lamina area (+), lumen breadth (+), t/b (−), and wood density (−) (Fig. 3b; Table S2) reflecting a hydraulic safety–efficiency spectrum. Like in the global PCA, PC2 (22.1%) was most strongly loaded by SLA (+) and LDMC (−), reflecting the leaf economics spectrum. At this site more than any other, the safety–efficiency spectrum (PC1) was almost completely orthogonal to the leaf economics spectrum (PC2) (Fig. 3b).

At the second driest site (760 mm yr^{-1}), which had the highest $\mathrm{Var}(\lambda)$ of 1.712, the loadings of all seven traits on PC1 (56.5%) were > |0.3| (Table S2). The strongest-loading traits were wood density (−), t/b (−), lumen breadth (+), and lamina area (+), similar to PC1 in the global PCA (compare Fig. 3a,c). PC2 (22.9%) was strongly loaded by SLA (+), LDMC (−), H_{max} (+), and lamina area (+) and captured remaining variation in the leaf economics spectrum not explained by PC1.

At mid west (830 mm yr^{-1}), which had the lowest $\mathrm{Var}(\lambda)$ of 0.716, PC1 (40.2%) again captured a safety–efficiency spectrum, but at this site LDMC contributed more equally to PC1 and PC2, showing stronger coordination with wood density than at other sites (Fig. 3d; Table S2). H_{max} and lamina area also loaded relatively strongly with SLA and LDMC on PC2 (23.5%). At the moderately mesic mid east site (912 mm yr^{-1}), PC1 (43.8%) again captured a
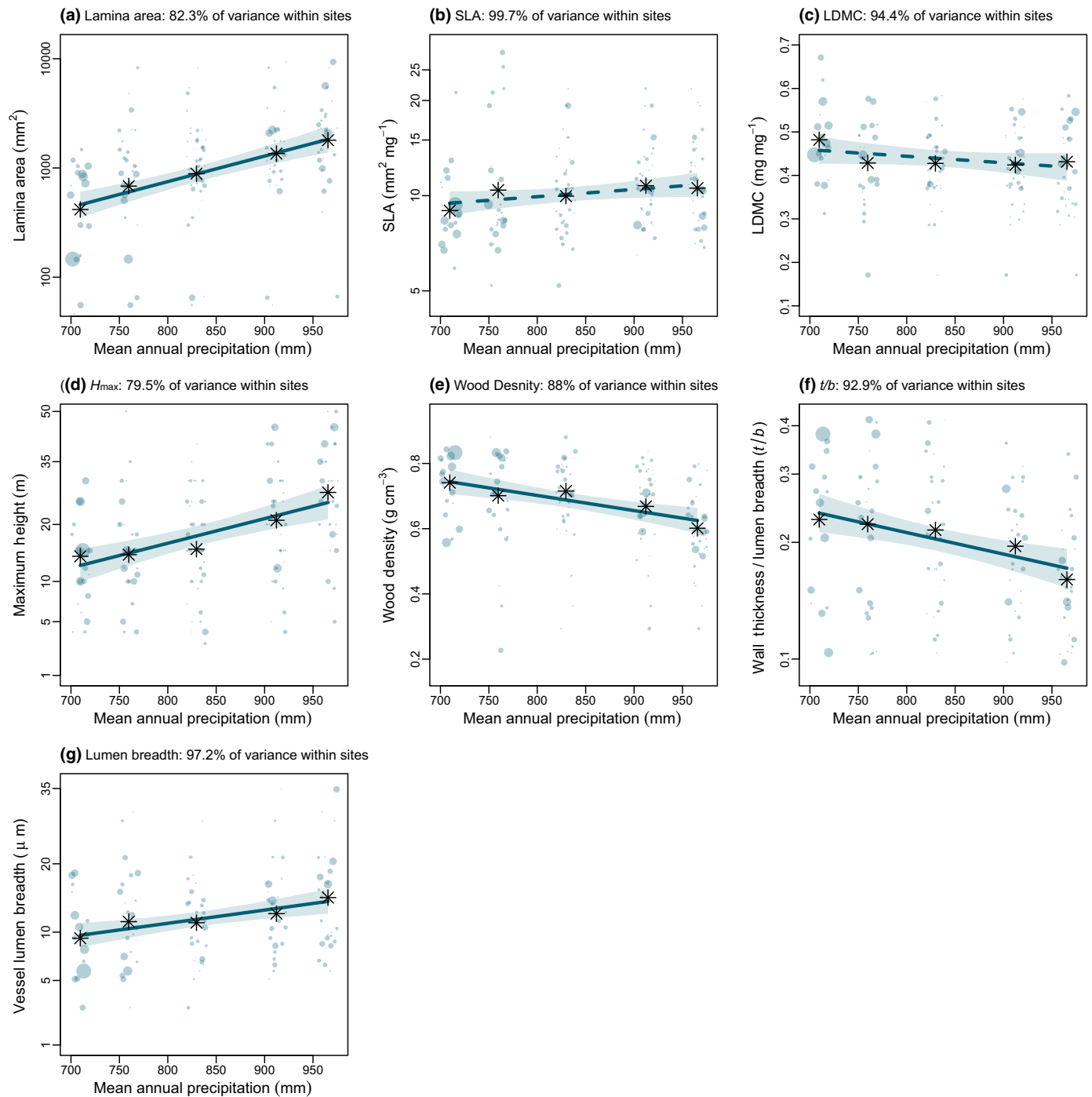
Fig. 1 Plots of each of the seven functional traits versus mean annual precipitation. Point sizes are proportional to the relative log(abundance + 1) of species in each site, and points have been jittered slightly for clarity. Asterisks are community-weighted means. Fitted lines are estimates of fixed-effects from linear mixed-effects models, and envelopes are associated 95% confidence intervals. Solid lines indicate significant ($\alpha = 0.05$) slopes, and dashed lines indicate nonsignificant slopes. Within-site variance components are also included for each trait. These were calculated using unweighted trait values in each site. LDMC, leaf dry matter content; SLA, specific leaf area.

safety–efficiency spectrum and PC2 captured the leaf economics spectrum (21.9%) (Fig. 3e; Table S2). H_{max} and lamina area also loaded relatively strongly with SLA and LDMC on PC2.

At the wettest site (965 mm yr^{-1}), PC1 (49.2%) was strongly loaded by maximum height (+), lamina area (+), lumen breadth (+), t/b (−), and wood density (−) (Fig. 3f; Table S2) reflecting a hydraulic safety–efficiency spectrum. Like in the global PCA, PC2 (21.4%) was most strongly loaded by SLA (+) and LDMC (−), reflecting the leaf economics spectrum. Lumen breadth also loaded strongly and positively on PC2.
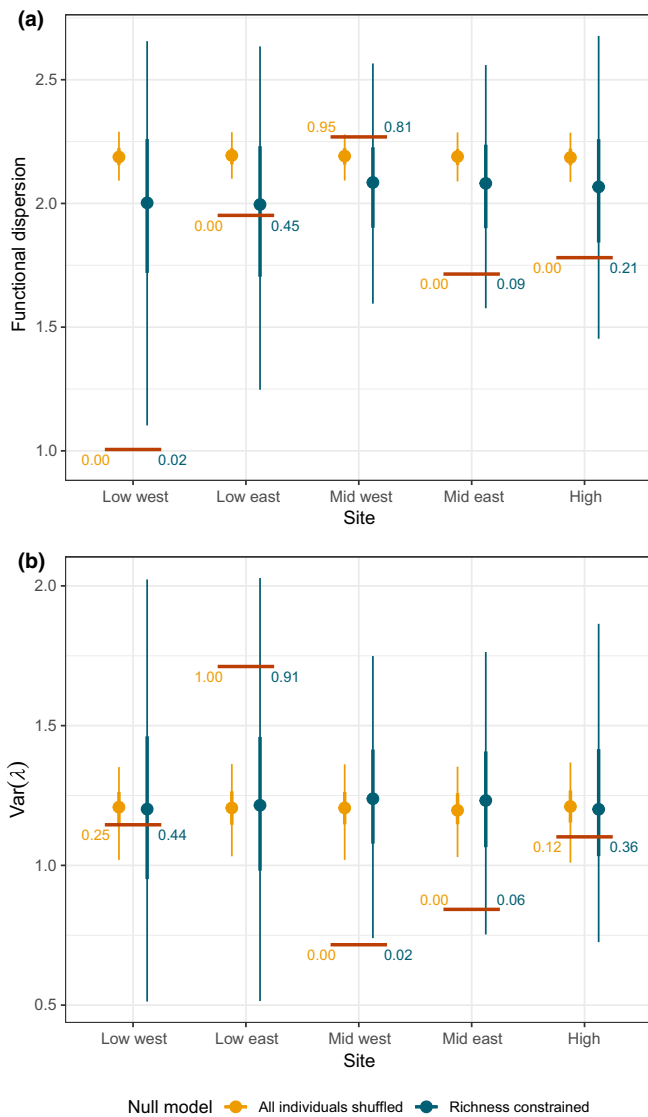
(a)

(b)

Null model: All individuals shuffled, Richness constrained

Fig. 2 Plots of observed and expected (a) functional dispersion and (b) Var (λ) values calculated for each site. In both plots the red horizontal bars are the observed values. The gold and blue points and vertical bars represent distributions from 999 permutations of the unconstrained and constrained null models, respectively. Points are medians, thick vertical bars span the 0.25 and 0.75 percentiles, and thin vertical bars span the 0.025 and 0.975 percentiles. The numbers are the percentiles where the observed values overlap the null model distributions. Values < 0.025 or > 0.975 can be interpreted as significant departures from null model expectations. Values of 0.00 or 1.00 indicate that the observed values were beyond the range of the null model distributions.

To further investigate the very high trait covariance at low east, and the unexpectedly lower trait covariance at the wettest and driest sites, we projected PC1 from low east through the assemblages of all other sites and visually compared communities along this axis (Fig. 4a). We also located each species on the global PC1 and visualized each assemblage along this global axis (Fig. 4b). The resulting plots were almost identical, indicating that both PCAs captured the same trait spectrum with their major axes. They revealed a predictable shift in strategies from the wettest to driest sites and confirmed a wide spread of trait combinations at

low east. These plots also revealed the presence of 'extreme' drought tolerators (e.g. *Alectryon diversifolius*) at the driest site, and the concomitant loss of drought avoiders (e.g. *Brachychiton discolor* and *D. photinophylla*) from this site (Fig. 4a). Other species of note included the generalist shrub *Alyxia ruscifolia*, which exhibited an extreme tolerator strategy despite being recorded in the understories of wetter sites, and *B. rupestris*, which exhibited an intermediate strategy along the tolerator–avoider spectrum at the driest site (Fig. 4a).

Discussion

Comprehensive assemblage and trait data from angiosperm communities across the Bunya Mountains revealed mixed support for our hypotheses. As hypothesized, CWMs for all traits but SLA and LDMC exhibited significant relationships with MAP. For the second hypothesis, FDis was lower than expected under random assembly at the driest site, but it did not increase consistently with MAP as hypothesized. Consistent with the third hypothesis, Var(λ) was lower than expected under random assembly in the middle site, but it did not peak at the wet and dry ends of the gradient. Instead, it peaked at the second driest site, where a wide spectrum of drought-resistance strategies was apparent, from shorter drought-tolerating species with safe hydraulics and small, robust leaves to taller species with efficient hydraulics and large leaves combined with drought-avoiding characteristics.

CWMs revealed trade-offs in average trait values along the gradient. As H_{max} increased so did average lamina area and lumen breadth, but these increases were associated with declines in average wood density and t/b. These results are largely consistent with studies of CWMs along precipitation gradients in rainforests elsewhere (Muscarella & Uriarte, 2016); but as Fig. 1 shows, the approach ignores a substantial amount of within-site variation and reveals little about the trade-offs operating *within* communities. Admittedly, the among-community trade-offs detected by CWMs were largely consistent with the within-community hydraulic trade-offs revealed by the major principal components at most sites.

Shifting hydraulic trade-offs along the moisture gradient

At the top of the range, adequate rainfall, cloud stripping, and cooler temperatures permit the development of taller forests driven by strong competition for light (King, 1990). To achieve the hydraulic efficiency required to overcome long path lengths, canopy species at this site had large vessel lumens and low–moderate wood density, which is consistent with coordination between height and hydraulics found globally (Liu *et al.*, 2019). Tall species also tended to have large leaves, though this trend was driven in part by a few large-leaved canopy species (e.g. *D. excelsa*, *B. discolor*, and *Diploglottis australis*), with most canopy species having near average-sized leaves. Taller species at this site also had low t/b values, indicating that even in the face of long path lengths they do not require well-reinforced petiole vessels to prevent loss of leaf hydraulic function via embolism (Blackman *et al.*, 2010). Though this site was the wettest on the
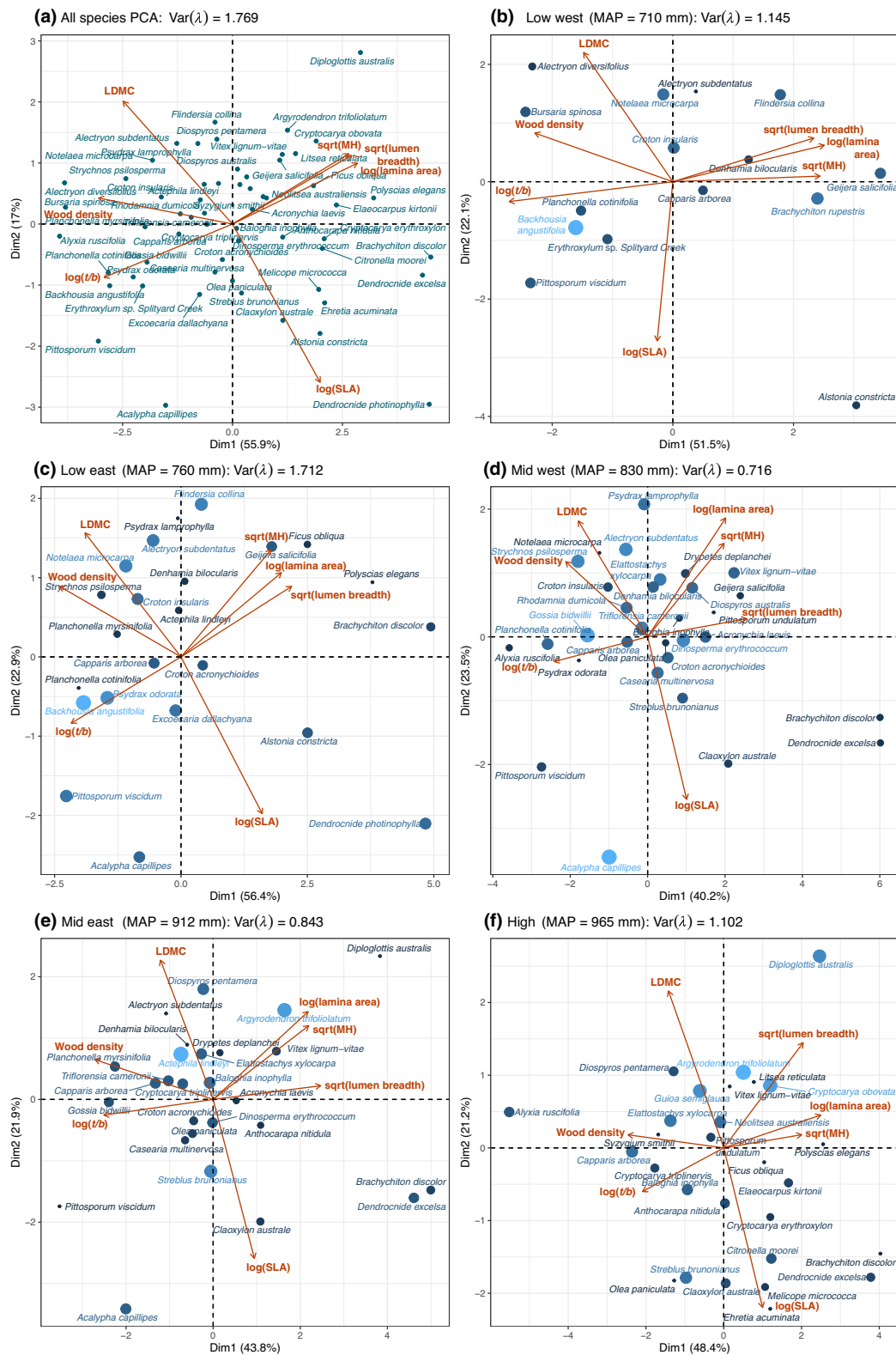
Fig. 3 Biplots from principal components analyses of the seven functional traits for (a) all species recorded across all sites (unweighted) and (b–f) species recorded in each site weighted by log(abundance + 1), with larger and lighter coloured points indicating more-abundant species. LDMC, leaf dry matter content; MH, maximum height; SLA, specific leaf area; t/b, vessel wall thickness/vessel lumen breadth.

Bunya Mountains, it is dry compared with rainforests globally (Malhi *et al.*, 2004) and the Australian subtropics specifically (Harwood *et al.*, 2016; BOM, 2021b). The Bunya Mountains

experience seasonal droughts during the region's drier spring months (BOM, 2021a) and are on the dry edge of the region's rainforest distribution. The same features that enable canopy
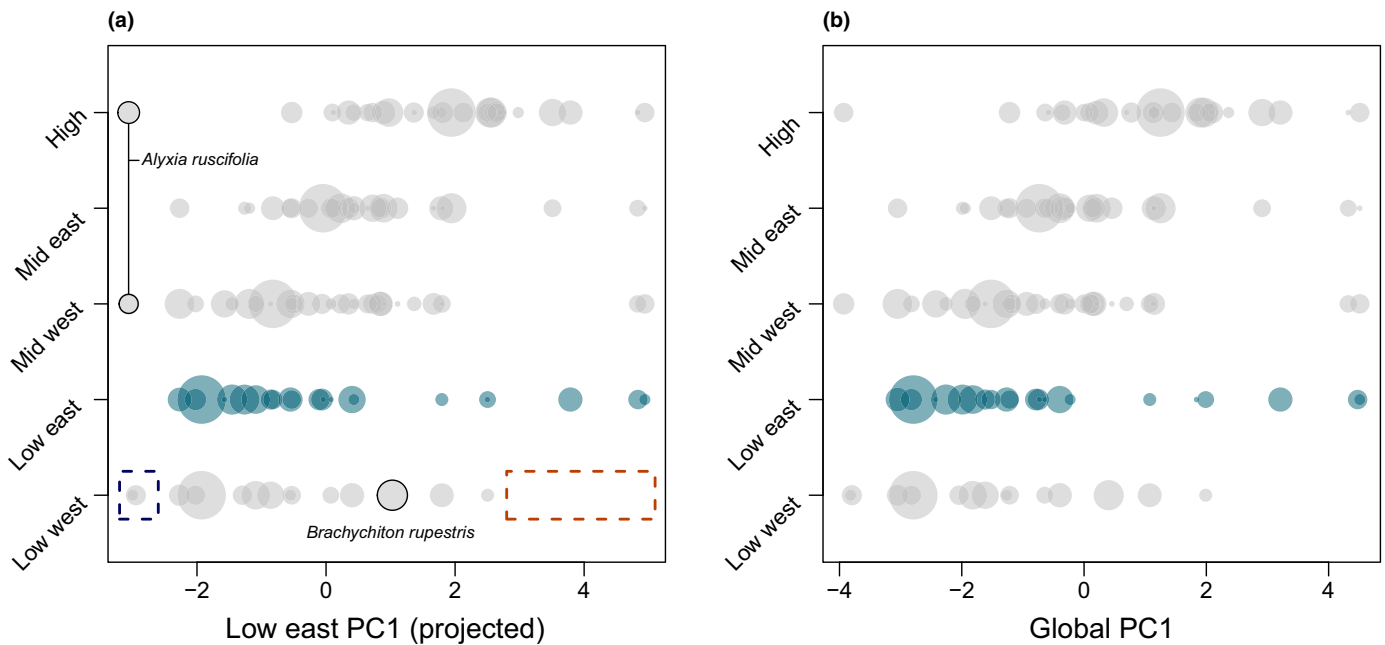
Fig. 4 Strip plots showing the position of species recorded in each site along (a) PC1 for low east (760 mm yr^{-1}) projected through each assemblage and (b) PC1 from the global principal components analysis. Point sizes are proportional to relative log(abundances), and teal points show assemblages for low east. The dashed rectangles in (a) highlight the emergence of 'extreme' drought tolerators (dark blue) and the loss of drought avoiders (red) at the driest site. Selected species referred to in the text are also highlighted in (a).

species to overcome long path lengths (moderate–low wood density and large vessel lumens) are probably also associated with high sapwood water content and capacitance (De Guzman *et al.*, 2020), which may allow these species to delay hydraulic stress by drawing on stored water reserves during seasonal droughts (Bartlett *et al.*, 2019). Comparisons with wetter rainforests in the region may reveal more variable strategies among canopy trees.

Compared with the wettest site, coordination between H_{max} and wood density weakened at the moderately mesic mid sites (second- and third-wettest sites) despite these sites sharing some canopy and understory species with the high site. At mid east, H_{max} loaded on both PC1 and PC2 and was somewhat decoupled from lumen breadth and wood density. This suggests that taller-growing species at this site invested more into hydraulic safety than at the most productive site. H_{max} was also positively correlated with LDMC on PC2, indicating that some tall species opted for robust leaves, likely in response to lower moisture availability (Scoffoni *et al.*, 2011). At mid west, coordination weakened among the measured traits, as indicated by the lowest Var (λ) value and significant departure from expected values under both randomization procedures. Interestingly, FDis was highest for this site, likely because weaker covariance among traits increases multivariate dispersion. Like at mid east, H_{max} was somewhat decoupled from lumen breadth and wood density, but LDMC was more strongly and positively related to wood density. This variable trait coordination was partly driven by the replacement of some tall, mesic canopy species (e.g. *Anthocarapa nitidula* and *Argyrodendron trofoliolatum*) with safer tree strategies (e.g. *Diospyros australis* and *Strychnos psilosperma*) and the co-occurrence of understory species with contrasting trait profiles

(e.g. the relatively efficient *Claoxylon australe* occurring with the safer *Croton insularis* and *Planchonella cotinifolia*). Accordingly, this site appears to represent a fulcrum along the moisture gradient where light and moisture limitation contribute somewhat equally to height-based trade-offs. Such shifts in the relative importance of light and water availability have been detected previously in the growth patterns of a generalist rainforest tree species distributed along moisture gradients in the tropics (Brienen *et al.*, 2010).

In the two driest sites we expected moisture limitation to dominate trait-based trade-offs, and this is indeed what we found. The very dominant PC1 at low east captured a strongly coordinated drought-tolerator–drought-avoider spectrum. Drought-tolerating species are evergreen and persist under low moisture conditions by reducing hydraulic conductance as water potentials decline, allowing them to maintain gas exchange (Bartlett *et al.*, 2019). An important leaf trait associated with drought tolerance in evergreen species is leaf turgor loss point π_{tlp} (Bartlett *et al.*, 2012; Kunert *et al.*, 2021). Though we did not include π_{tlp} in the analyses reported earlier herein, measurements were taken on a subset of species that revealed a strong negative correlation with LDMC (Fig. S5), as has been reported previously in angiosperms (Bartlett *et al.*, 2012; Laughlin *et al.*, 2020). We are therefore confident that our measured traits captured drought-tolerating strategies at the leaf level, albeit indirectly. Exemplary drought-tolerating species at low east included *P. cotinifolia*, *B. angustifolia*, and *Notelaea microcarpa*. At the other end of the spectrum, drought-avoiding species persist under low moisture conditions by maintaining high water content to allow hydraulic conductance to decline more slowly with increasingly negative water

potentials (Choat *et al.*, 2005; Bartlett *et al.*, 2019). Traits associated with drought avoidance include leaf shedding, high sapwood water content, and connected and conductive xylem to facilitate capacitance (Meinzer *et al.*, 2009). Again, these traits were not measured directly in this study but were captured by measuring wood density (related to sapwood water storage and capacitance; Meinzer *et al.*, 2003; De Guzman *et al.*, 2020), vessel lumen breadths (Choat *et al.*, 2005), and leaf traits related to leaf lifespan and construction costs (Markesteijn *et al.*, 2011). The most extreme expressions of this strategy at low east included *B. discolor* and *D. photinophylla*. We note that *B. discolor* was present at wetter sites also, indicating that its strategy is viable for dealing with both light competition in taller productive sites and water limitation in drier sites.

At the driest site, Var(λ) was lower than at low east due to the truncation of the tolerator–avoider spectrum. This was also reflected in the very low FDis, which is consistent with a strong contraction of trait space at the driest site. Of note was the apparent replacement of *B. discolor* with its congener *B. rupestris*. *Brachychiton rupestris* is a semiarid-adapted pachycaul that combines its impressive water storage capacity (an avoiding strategy) with drought-tolerating leaf traits, including small lamina area (an order of magnitude smaller than *B. discolor*), low SLA (2.6 times lower than *B. discolor*), and intermediate petiole lumen breadths (3.5 times smaller than *B. discolor*). The combination of traits related to drought avoidance and tolerance found in this study is consistent with a comparative study of *Brachychiton* species that identified a combination of avoiding and tolerating strategies in other traits for *B. rupestris* seedlings, including the ability to increase water use efficiency under experimental drought (Reynolds *et al.*, 2017).

The absence of archetypal drought avoiders at the driest site, without the co-occurring drought-tolerating traits seen in *B. rupestris*, indicates that a classic drought-avoidance strategy is only viable up to a limit of drought severity and duration, beyond which the strategy cannot avoid excessive cellular damage (Claeys & Inzé, 2013). Unlike safe hydraulic strategies that resist embolism through the structural features of xylem, avoiders employ leaf shedding combined with water storage and capacitance to minimize water loss and limit fluctuations in xylem tension (Meinzer *et al.*, 2009) and therefore operate with smaller hydraulic safety margins than drought tolerators (Choat *et al.*, 2012). This strategy is likely to perform poorly under prolonged drought if stored water sources are depleted and there is insufficient annual precipitation to replenish stored water. Across a range of deciduous and evergreen species from the Sonoran Desert, Pockman & Sperry (2000) found that hydraulic safety margins were correlated with the variability of water availability, where smaller safety margins were associated with riparian habitats with more consistent water supply. Low predictability of precipitation could also contribute to their absence at the driest site, especially drought-deciduous species that attempt to anticipate rainfall by flushing (initiating re-leafing) before the onset of seasonal rainfall (Eamus, 1999; Méndez-Alonzo *et al.*, 2013). Frost incidence is also known to apply a strong habitat filter on leaf size (Wright *et al.*, 2017), but frost days are more common at the higher, wetter sites (Table 1), making it unlikely that frosts contribute to the filtering of large-leaved avoiders from the driest site in this system.

Trait covariance Var(λ) and species richness

Dwyer & Laughlin (2017) hypothesized that within-community trait covariance strengthens with environmental stress; in turn, species richness declines as trait covariance increases due to increasing constraints on viable trait combinations. Though support for all or part of this hypothesis has since been reported in a range of systems (Dwyer & Laughlin, 2017; Delhaye *et al.*, 2020; Silva *et al.*, 2021; Xing *et al.*, 2021; Sanaphre-Villanueva *et al.*, 2022), we did not expect support for this hypothesis at the Bunya Mountains for several reasons. First, we expected H_{max} to be coordinated with hydraulic traits in a similar manner at both the wettest and driest ends of our gradient, because light- and moisture-driven trade-offs involving H_{max} are not mutually exclusive (Sterck *et al.*, 2006; Markesteijn *et al.*, 2011; Liu *et al.*, 2019). Second, we did not necessarily expect species richness to increase with MAP along the gradient because diversity patterns at the Bunya Mountains are thought to be strongly influenced by biogeographic processes (Butler, 2004). In particular, the CNVFs in which our wettest site was located are spatially isolated from other areas with similar climatic and edaphic niches. The closest similar niches occur *c.* 130 km to the southeast of the Bunya Mountains at Main Range. By contrast, the notophyll vine forests in which we sampled our 'mid' sites are well represented just 20 km away in the formerly extensive forests around Yarraman. Thus, high-altitude forests may be considered a regional sink where dispersal is low and extinction is high, leading to relatively low species richness, whereas much higher regional connectivity appears to prevent local extinctions in the mid-altitude forests leading to similar rarefied richness at both 'high' and 'mid' sites (Fig. S6).

Conclusion

This study revealed trade-offs related to hydraulic strategies at both the wettest and driest ends of a steep orographic moisture gradient at the Bunya Mountains. Traits coordinated most strongly along an axis of drought tolerance to drought avoidance in moderately dry locations, but less so in the driest location where drought-avoiding strategies become less viable due to insufficient or unpredictable rainfall. This study also highlights how analyses of trait covariance, combined with traditional univariate and multivariate trait-based approaches, can reveal complementary information about processes structuring plant communities. Future research should focus on coordination of hydraulic traits from the subtropics to the tropics in eastern Australia to examine how rainfall amount and seasonality influences coordination of species along the drought tolerance–avoidance spectrum (Choat *et al.*, 2005). A greater understanding of these abiotic constraints will improve predictions of species vulnerable to ongoing climate change and inform the selection of species assemblages for restoration projects that are ready to meet the challenges of future climates.

Author contributions

AB surveyed two of five sites, measured most traits, undertook all preliminary analyses, and drafted the preliminary manuscript with assistance from JMD; DB surveyed three of five sites; JR-S assisted AB with fieldwork and contributed additional traits to expand trait coverage; JMD revised analyses and the manuscript prior to submission, with input from all authors.

ORCID

Donald W. Butler https://orcid.org/0000-0002-6019-1078
John M. Dwyer https://orcid.org/0000-0001-7389-5528
Julian Radford-Smith https://orcid.org/0000-0001-6949-9469

Data availability

'Bunyas R Project' including all data and scripts to reproduce analyses, figures, and tables is available on Dryad doi: 10.5061/dryad.rbnzs7hdt.

References

Baas P, Ewers FW, Davis SD, Wheeler EA. 2004. 15 – Evolution of xylem physiology. In: Hemsley AR, Poole I, eds. *The evolution of plant physiology.* Oxford, UK: Academic Press, 273–295.

Bartlett MK, Detto M, Pacala SW. 2019. Predicting shifts in the functional composition of tropical forests under increased drought and CO_2 from trade-offs among plant hydraulic traits. *Ecology Letters* 22: 67–77.

Bartlett MK, Scoffoni C, Ardy R, Zhang Y, Sun S, Cao K, Sack L. 2012. Rapid determination of comparative drought tolerance traits: using an osmometer to predict turgor loss point. *Methods in Ecology and Evolution* 3: 880–888.

Bartomeus I. 2019. FUNDIV. R package beta version. [WWW document] URL https://github.com/ibartomeus/fundiv [accessed 4 December 2021].

Bates D, Mächler M, Bolker B, Walker S. 2015. Fitting linear mixed-effects models using LME4. *Journal of Statistical Software* 67: 48.

Blackman CJ, Brodribb TJ, Jordan GJ. 2010. Leaf hydraulic vulnerability is related to conduit dimensions and drought resistance across a diverse range of woody angiosperms. *New Phytologist* 188: 1113–1123.

Blackman CJ, Gleason SM, Cook AM, Chang Y, Laws CA, Westoby M. 2018. The links between leaf hydraulic vulnerability to drought and key aspects of leaf venation and xylem anatomy among 26 Australian woody angiosperms from contrasting climates. *Annals of Botany* 122: 59–67.

Blonder B, Lamanna C, Violle C, Enquist BJ. 2014. The *n*-dimensional hypervolume. *Global Ecology and Biogeography* 23: 595–609.

BOM (Australian Bureau of Meteorology). 2021a. *Climate data for Mt Mowbullan (station no. 040435).* Canberra, ACT, Australia: Australian Bureau of Meteorology.

BOM (Australian Bureau of Meteorology). 2021b. *Climate data for Springbrook Road (station no. 40607).* Canberra, ACT, Australia: Australian Bureau of Meteorology.

Boucher FC, Thuiller W, Arnoldi C, Albert CH, Lavergne S. 2013. Unravelling the architecture of functional variability in wild populations of *Polygonum viviparum* L. *Functional Ecology* 27: 382–391.

Brienen RJW, Zuidema PA, Martínez-Ramos M. 2010. Attaining the canopy in dry and moist tropical forests: strong differences in tree growth trajectories reflect variation in growing conditions. *Oecologia* 163: 485–496.

Bruelheide H, Dengler J, Purschke O, Lenoir J, Jiménez-Alfaro B, Hennekens SM, Botta-Dukát Z, Chytrý M, Field R, Jansen F et al. 2018. Global trait–environment relationships of plant communities. *Nature Ecology & Evolution* 2: 1906–1917.

Butler DW. 2004. *Seed dispersal syndromes and the distribution of woody plants in South-East Queensland's vine-forests.* PhD thesis, The University of Queensland, Australia.

Cheverud JM, Wagner GP, Dow MM. 1989. Methods for the comparative analysis of variation patterns. *Systematic Zoology* 38: 201–213.

Choat B, Ball MC, Luly JG, Holtum JAM. 2005. Hydraulic architecture of deciduous and evergreen dry rainforest tree species from north-eastern Australia. *Trees* 19: 305–311.

Choat B, Jansen S, Brodribb TJ, Cochard H, Delzon S, Bhaskar R, Bucci SJ, Feild TS, Gleason SM, Hacke UG et al. 2012. Global convergence in the vulnerability of forests to drought. *Nature* 491: 752–755.

Claeys H, Inzé D. 2013. The agony of choice: how plants balance growth and survival under water-limiting conditions. *Plant Physiology* 162: 1768–1779.

Cornwell WK, Ackerly DD. 2009. Community assembly and shifts in plant trait distributions across an environmental gradient in coastal California. *Ecological Monographs* 79: 109–126.

De Guzman ME, Acosta-Rangel A, Winter K, Meinzer FC, Bonal D, Santiago LS. 2020. Hydraulic traits of Neotropical canopy liana and tree species across a broad range of wood density: implications for predicting drought mortality with models. *Tree Physiology* 41: 24–34.

Delhaye G, Bauman D, Séleck M, Ilunga wa Ilunga E, Mahy G, Meerts P. 2020. Interspecific trait integration increases with environmental harshness: a case study along a metal toxicity gradient. *Functional Ecology* 34: 1428–1437.

Dwyer JM, Laughlin DC. 2017. Constraints on trait combinations explain climatic drivers of biodiversity: the importance of trait covariance in community assembly. *Ecology Letters* 20: 872–882.

Eamus D. 1999. Ecophysiological traits of deciduous and evergreen woody species in the seasonally dry tropics. *Trends in Ecology & Evolution* 14: 11–16.

Falster DS, Brännström Å, Westoby M, Dieckmann U. 2017. Multitrait successional forest dynamics enable diverse competitive coexistence. *Proceedings of the National Academy of Sciences, USA* 114: E2719–E2728.

Funk JL, Cornwell WK. 2013. Leaf traits within communities: context may affect the mapping of traits to function. *Ecology* 94: 1893–1897.

Gleason SM, Westoby M, Jansen S, Choat B, Hacke UG, Pratt RB, Bhaskar R, Brodribb TJ, Bucci SJ, Cao K-F et al. 2016. Weak tradeoff between xylem safety and xylem-specific hydraulic efficiency across the world's woody plant species. *New Phytologist* 209: 123–136.

Harden GJ, McDonald WJF, Williams JB. 2006. *Rainforest trees and shrubs: a field guide to their identification.* Nambucca Heads, NSW, Australia: Gwen Harden.

Harwood T, Donohue R, Harman I, McVicar T, Ota N, Perry J, Williams K. 2016. *9s climatology for continental Australia 1976–2005: summary variables with elevation and radiative adjustment v.3.* Canberra, ACT, Australia: CSIRO Data Collection.

Hietz P, Rosner S, Hietz-Seifert U, Wright SJ. 2017. Wood traits related to size and life history of trees in a Panamanian rainforest. *New Phytologist* 213: 170–180.

Hijmans RJ. 2021. RASTER: geographic data analysis and modeling. R package v.3.4-13. [WWW document] URL https://CRAN.R-project.org/package=raster

Hutchinson MF, Xu T, Kesteven JL, Marang IJ, Evans BJ. 2022. *ANUClimate v.2.0.* Canberra, ACT, Australia: NCI Australia.

Ilic J, Boland D, McDonald M, Downes D, Blakemore P. 2000. *Woody density phase 1 – state of knowledge.* Canberra, ACT, Australia: Australian Greenhouse Office.

King DA. 1990. The adaptive significance of tree height. *The American Naturalist* 135: 809–828.

Koch GW, Sillett SC, Jennings GM, Davis SD. 2004. The limits to tree height. *Nature* 428: 851–854.

Kraft NJB, Adler PB, Godoy O, James EC, Fuller S, Levine JM. 2015. Community assembly, coexistence and the environmental filtering metaphor. *Functional Ecology* 29: 592–599.

Kunert N, Zailaa J, Herrmann V, Muller-Landau HC, Wright SJ, Pérez R, McMahon SM, Condit RC, Hubbell SP, Sack L *et al.* 2021. Leaf turgor loss point shapes local and regional distributions of evergreen but not deciduous tropical trees. *New Phytologist* 230: 485–496.

Laliberté E, Legendre P. 2010. A distance-based framework for measuring functional diversity from multiple traits. *Ecology* 91: 299–305.

Laughlin DC, Delzon S, Clearwater MJ, Bellingham PJ, McGlone MS, Richardson SJ. 2020. Climatic limits of temperate rainforest tree species are explained by xylem embolism resistance among angiosperms but not among conifers. *New Phytologist* 226: 727–740.

Laughlin DC, Fule PZ, Huffman DW, Crouse J, Laliberte E. 2011. Climatic constraints on trait-based forest assembly. *Journal of Ecology* 99: 1489–1499.

Laughlin DC, Joshi C, van Bodegom PM, Bastow ZA, Fulé PZ. 2012. A predictive model of community assembly that incorporates intraspecific trait variation. *Ecology Letters* 15: 1291–1299.

Lê S, Josse J, Husson F. 2008. FactoMineR: an R package for multivariate analysis. *Journal of Statistical Software* 25: 1–18.

Leigh A, Sevanto S, Close JD, Nicotra AB. 2017. The influence of leaf size and shape on leaf thermal dynamics: does theory hold up under natural conditions? *Plant, Cell & Environment* 40: 237–248.

Liang X, Ye Q, Liu H, Brodribb TJ. 2021. Wood density predicts mortality threshold for diverse trees. *New Phytologist* 229: 3053–3057.

Liu H, Gleason SM, Hao G, Hua L, He P, Goldstein G, Ye Q. 2019. Hydraulic traits are coordinated with maximum plant height at the global scale. *Science Advances* 5: eaav1332.

Liu H, Ye Q, Gleason SM, He P, Yin D. 2021. Weak tradeoff between xylem hydraulic efficiency and safety: climatic seasonality matters. *New Phytologist* 229: 1440–1452.

Lohbeck M, Lebrija-Trejos E, Martínez-Ramos M, Meave JA, Poorter L, Bongers F. 2015. Functional trait strategies of trees in dry and wet tropical forests are similar but differ in their consequences for succession. *PLoS ONE* 10: e0123741.

Lowman M, Box JD. 1983. Variation in leaf toughness and phenolic content among five species of Australian rain forest trees. *Austral Ecology* 8: 17–25.

Malhi Y, Phillips OL, Malhi Y, Wright J. 2004. Spatial patterns and recent trends in the climate of tropical rainforest regions. *Philosophical Transactions of the Royal Society of London. Series B: Biological Sciences* 359: 311–329.

Markesteijn L, Poorter L, Bongers F, Paz H, Sack L. 2011. Hydraulics and life history of tropical dry forest tree species: coordination of species' drought and shade tolerance. *New Phytologist* 191: 480–495.

Marks CO, Lechowicz MJ. 2006. Alternative designs and the evolution of functional diversity. *The American Naturalist* 167: 55–66.

McCarthy JK, Dwyer JM, Mokany K. 2019. A regional-scale assessment of using metabolic scaling theory to predict ecosystem properties. *Proceedings of the Royal Society B: Biological Sciences* 286: 20192221.

McGill BJ, Enquist BJ, Weiher E, Westoby M. 2006. Rebuilding community ecology from functional traits. *Trends in Ecology & Evolution* 21: 178–185.

Meinzer FC, James SA, Goldstein G, Woodruff D. 2003. Whole-tree water transport scales with sapwood capacitance in tropical forest canopy trees. *Plant, Cell & Environment* 26: 1147–1155.

Meinzer FC, Johnson DM, Lachenbruch B, McCulloh KA, Woodruff DR. 2009. xylem hydraulic safety margins in woody plants: coordination of stomatal control of xylem tension with hydraulic capacitance. *Functional Ecology* 23: 922–930.

Méndez-Alonzo R, Pineda-García F, Paz H, Rosell JA, Olson ME. 2013. Leaf phenology is associated with soil water availability and xylem traits in a tropical dry forest. *Trees* 27: 745–754.

Messier J, Lechowicz MJ, McGill BJ, Violle C, Enquist BJ. 2017. Interspecific integration of trait dimensions at local scales: the plant phenotype as an integrated network. *Journal of Ecology* 105: 1775–1790.

Muscarella R, Uriarte M. 2016. Do community-weighted mean functional traits reflect optimal strategies? *Proceedings of the Royal Society B: Biological Sciences* 283: 20152434.

Niklas KJ. 1992. *Plant biomechanics: an engineering approach to plant form and function.* Chicago, IL, USA: University of Chicago Press.

Oksanen J, Blanchet FG, Kindt R, Legendre P, Minchin PR, O'Hara RB, Simpson GL, Solymos P, Stevens MH, Wagner H. 2021. vegan: community ecology package. R package v.2.5-7. [WWW document] URL http://CRAN.R-project.org/package=vegan

Pineda-García F, Paz H, Meinzer FC. 2013. Drought resistance in early and late secondary successional species from a tropical dry forest: the interplay between xylem resistance to embolism, sapwood water storage and leaf shedding. *Plant, Cell & Environment* 36: 405–418.

Pockman WT, Sperry JS. 2000. Vulnerability to xylem cavitation and the distribution of sonoran desert vegetation. *American Journal of Botany* 87: 1287–1299.

Poorter L. 2009. Leaf traits show different relationships with shade tolerance in moist versus dry tropical forests. *New Phytologist* 181: 890–900.

Queensland Herbarium. 2015. *Regional Ecosystem Description Database (REDD), v.9.0 (April 2015).* Brisbane, Qld, Australia: DSITI.

R Development Core Team. 2021. *R: a language and environment for statistical computing.* Vienna, Austria: R Foundation for Statistical Computing. [WWW document] URL http://www.R-project.org/ [accessed 3 September 2021].

Raymond OL, Liu S, Gallagher R, Zhang W, Highet LM. 2012. *Surface Geology of Australia 1:1 million scale dataset 2012 edition.* Canberra, ACT, Australia: Geoscience Australia. [WWW document] URL http://pid.geoscience.gov.au/dataset/ga/74619 [accessed 9 June 2022].

Reynolds VA, Anderegg LDL, Loy X, HilleRisLambers J, Mayfield MM. 2017. Unexpected drought resistance strategies in seedlings of four *Brachychiton* species. *Tree Physiology* 38: 1–14.

Ryan MG, Yoder BJ. 1997. Hydraulic limits to tree height and tree growth. *Bioscience* 47: 235–242.

Sanaphre-Villanueva L, Pineda-García F, Dáttilo W, Pinzón-Pérez LF, Ricaño-Rocha A, Paz H. 2022. Above- and below-ground trait coordination in tree seedlings depend on the most limiting resource: a test comparing a wet and a dry tropical forest in Mexico. *PeerJ* 10: e13458.

Schneider CA, Rasband WS, Eliceiri KW. 2012. NIH Image to ImageJ: 25 years of image analysis. *Nature Methods* 9: 671–675.

Scoffoni C, Rawls M, McKown A, Cochard H, Sack L. 2011. Decline of leaf hydraulic conductance with dehydration: relationship to leaf size and venation architecture. *Plant Physiology* 156: 832–843.

Shipley B, Vile D, Garnier E. 2006. From plant traits to plant communities: a statistical mechanistic approach to biodiversity. *Science* 314: 812–814.

Silva JLA, Souza AF, Vitória AP. 2021. Leaf trait integration mediates species richness variation in a species-rich neotropical forest domain. *Plant Ecology* 222: 1183–1195.

Spasojevic MJ, Grace JB, Harrison S, Damschen EI. 2014. Functional diversity supports the physiological tolerance hypothesis for plant species richness along climatic gradients. *Journal of Ecology* 102: 447–455.

Spasojevic MJ, Suding KN. 2012. Inferring community assembly mechanisms from functional diversity patterns: the importance of multiple assembly processes. *Journal of Ecology* 100: 652–661.

Sterck F, Markesteijn L, Schieving F, Poorter L. 2011. Functional traits determine trade-offs and niches in a tropical forest community. *Proceedings of the National Academy of Sciences, USA* 108: 20627–20632.

Sterck FJ, Poorter L, Schieving F. 2006. Leaf traits determine the growth-survival trade-off across rain forest tree species. *The American Naturalist* 167: 758–765.

Tyree MT, Zimmerman MH. 2002. *Xylem structure and the ascent of sap.* Heidelberg, Germany: Springer.

Villéger S, Mason NWH, Mouillot D. 2008. New multidimensional functional diversity indices for a multifaceted framework in functional ecology. *Ecology* **89**: 2290–2301.

Weiher E, Keddy PA. 1995. Assembly rules, null models, and trait dispersion – new questions front old patterns. *Oikos* **74**: 159–164.

Westoby M, Falster DS, Moles AT, Vesk PA, Wright IJ. 2002. Plant ecological strategies: some leading dimensions of variation between species. *Annual Review of Ecology, Evolution, and Systematics* **33**: 125–159.

Williamson GB, Wiemann MC. 2010. Measuring wood specific gravity. . .correctly. *American Journal of Botany* **97**: 519–524.

Wright IJ, Dong N, Maire V, Prentice IC, Westoby M, Díaz S, Gallagher RV, Jacobs BF, Kooyman R, Law EA et al. 2017. Global climatic drivers of leaf size. *Science* **357**: 917–921.

Wright SJ, Kitajima K, Kraft NJB, Reich PB, Wright IJ, Bunker DE, Condit R, Dalling JW, Davies SJ, Díaz S et al. 2010. Functional traits and the growth–mortality trade-off in tropical trees. *Ecology* **91**: 3664–3674.

Xing K, Niinemets Ü, Rengel Z, Onoda Y, Xia J, Chen HYH, Zhao M, Han W, Li H. 2021. Global patterns of leaf construction traits and their covariation along climate and soil environmental gradients. *New Phytologist* **232**: 1648–1660.

Zach A, Schuldt B, Brix S, Horna V, Culmsee H, Leuschner C. 2010. Vessel diameter and xylem hydraulic conductivity increase with tree height in tropical rainforest trees in Sulawesi, Indonesia. *Flora – Morphology, Distribution, Functional Ecology of Plants* **205**: 506–512.

Supporting Information

Additional Supporting Information may be found online in the Supporting Information section at the end of the article.

Fig. S1 Site locations.

Fig. S2 Images of petiole xylem vessels.

Fig. S3 Wood density regression (80°C vs 105°C).

Fig. S4 Trait variance components.

Fig. S5 Pairwise scatterplots measured traits and leaf turgor loss point.

Fig. S6 Richness plots.

Table S1 Trait coverage table.

Table S2 Trait loadings from principal component analyses for each site.

Please note: Wiley Blackwell are not responsible for the content or functionality of any Supporting Information supplied by the authors. Any queries (other than missing material) should be directed to the *New Phytologist* Central Office.